Impact of Common Epidermal Growth Factor Receptor and HER2 Variants on Receptor Activity and Inhibition by Lapatinib

Tona M. Gilmer,[1] Louann Cable,[1] Krystal Alligood,[1] David Rusnak,[1] Glenn Spehar,[2] Kathleen T. Gallagher,[5] Ermias Woldu,[5] H. Luke Carter,[3] Anne T. Truesdale,[3] Lisa Shewchuk,[4] and Edgar R. Wood[3]

Departments of [1]Translational Medicine, [2]Oncology Biology, [3]Biochemical and Cellular Targets, and [4]Computational, Analytical, and Structural Sciences; and [5]Discovery Technology Group, GlaxoSmithKline, Collegeville, Pennsylvania and Research Triangle Park, North Carolina

Abstract

The goal of this study was to characterize the effects of non–small cell lung carcinoma (NSCLC)-associated mutations in epidermal growth factor receptor (*EGFR/ErbB1*) and *HER2* (*ErbB2*) on interactions with the dual tyrosine kinase inhibitor lapatinib. Biochemical studies show that commonly observed variants of EGFR [G719C, G719S, L858R, L861Q, and Δ746–750 (del15)] are enzyme activating, increasing the tyrosine kinase V_{max} and increasing the $K_m^{(app)}$ for ATP. The point mutations G719C and L861Q had minor effects on lapatinib K_is, whereas EGFR mutations L858R and del15 had a higher K_i for lapatinib than wild-type EGFR. Structural analysis of wild-type EGFR-lapatinib complexes and modeling of the EGFR mutants were consistent with these data, suggesting that loss of structural flexibility and possible stabilization of the active-like conformation could interfere with lapatinib binding, particularly to the EGFR deletion mutants. Furthermore, EGFR deletion mutants were relatively resistant to lapatinib-mediated inhibition of receptor autophosphorylation in recombinant cells expressing the variants, whereas EGFR point mutations had a modest or no effect. Of note, EGFR T790M, a receptor variant found in patients with gefitinib-resistant NSCLC, was also resistant to lapatinib-mediated inhibition of receptor autophosphorylation. Two HER2 insertional variants found in NSCLC were less sensitive to lapatinib inhibition than two HER2 point mutants. The effects of lapatinib on the proliferation of human NSCLC tumor cell lines expressing wild-type or variant EGFR and HER2 cannot be explained solely on the basis of the biochemical activity or receptor autophosphorylation in recombinant cells. These data suggest that cell line genetic heterogeneity and/or multiple determinants modulate the role played by EGFR/HER2 in regulating cell proliferation. [Cancer Res 2008;68(2):571–9]

Introduction

Several years of clinical experience with targeted tyrosine kinase inhibitors have shown that the efficacy of these compounds in the clinic is variable and difficult to predict with high accuracy (1–12). It is reasonable to propose that such variation in efficacy reflects genetic heterogeneity in the tumors of treated patients, and recent evidence strongly supports this possibility. For example, the ability to respond to selective kinase inhibitors, such as gefitinib, erlotinib, and imatinib, has been correlated with mutations in the target receptor (13–16). Detailed studies with gefitinib-responsive (non–small cell lung carcinoma) NSCLC patients showed that gefitinib efficacy is linked to activating mutations in the epidermal growth factor receptor (*EGFR*) that sensitize the tumor to the drug, possibly by stimulating drug-induced apoptosis (17). A causal relationship between *EGFR* genotype and drug susceptibility is also supported by the fact that some drug-resistant alleles carry second-site mutations that seem to act as suppressors of *EGFR*-activating, drug-sensitizing mutations (18, 19). Similar observations have also been made for chronic myelogenous leukemia and gastrointestinal stromal tumors–derived cells that acquire resistance to imatinib (20).

A number of *EGFR* mutations have been described that are enriched in NSCLC adenocarcinomas and in female never smokers of Asian ethnicity (21). The *EGFR* mutations include in-frame deletions affecting residues 746 to 753, multiple isolates of *EGFR*-L858R, and other point mutations in exons 18 to 21 (11). *EGFR*-T790M is a second-site mutation that has been reported in several NSCLC tumors that is strongly associated with resistance to gefitinib (19). Similar mutational patterns have been reported in *HER2*, and Shigematsu and coworkers (22) recently reported that 11 of 671 (1.6%) of patients' tumors contained *HER2* mutant alleles in a study of NSCLC. As observed for *EGFR*, the mutations included primarily in-frame mutations in exon 20 and were highly enriched in adenocarcinomas in female never smokers of Asian ethnicity.

Cell-based studies suggest that the sensitizing mutations in EGFR potentiate the ability of epidermal growth factor (EGF) to activate the receptor, and that the activated mutant EGFR is more susceptible to drug-dependent inhibition (11, 17, 18). This is consistent with the fact that the activating mutations are located in the tyrosine kinase domain and cluster in or near the ATP binding pocket of EGFR. Cell-based studies typically measure the steady-state level of receptor phosphorylation on tyrosine, so it is currently unclear if the mutations result in enhanced kinase activity, enhanced activation by ligand, or reduced down-regulation. Biochemical studies with purified receptors and structural studies, including cocrystals with inhibitors, are needed to understand the mechanism by which these mutations alter clinical outcome for different drugs and different cancers.

Lapatinib, erlotinib, and gefitinib are members of the 4-anilinoquinazoline group of tyrosine kinase inhibitiors. Although erlotinib and gefitinib are specific inhibitors of EGFR, lapatinib is a

Note: Supplementary data for this article are available at Cancer Research Online (http://cancerres.aacrjournals.org/).

Present address for G. Spehar: Adherex Technologies, Durham, NC 27703.

Requests for reprints: Tona M. Gilmer, Department of Translational Medicine, GlaxoSmithKline, 5 Moore Drive, Research Triangle Park, NC 27709. Phone: 919-483-2100; Fax: 919-315-3749; E-mail: tona.m.gilmer@gsk.com.

doi:10.1158/0008-5472.CAN-07-2404

p.o. potent dual inhibitor of EGFR (ErbB1) and HER2 (ErbB2; refs. 23, 24) that strongly down-regulates the antiapoptotic Akt pathway in responsive cells (25). Biochemical studies show that the EGFR-lapatinib complex has a long half-life and is characterized by a much slower dissociation rate than the erlotinib- or gefitinib-receptor complexes (24). This mode of binding may potentiate drug efficacy by prolonging drug-induced down-regulation of receptor-mediated tyrosine kinase activity. Indeed, lapatinib has shown clinical benefit for the treatment of metastatic breast cancers that overexpress HER2 when given alone or in combination with chemotherapy (26, 27) and was recently approved by the Food and Drug Administration for the treatment of patients with advanced or metastatic breast cancer whose tumors overexpress HER2.

The goal of this study was to characterize the interactions of lapatinib with wild-type EGFR and several of the common mutant variants of EGFR observed in NSCLC. For comparison, receptor variants were also challenged with gefitinib. In addition, the effect of lapatinib on four variants of HER2 was also examined. The results presented here reveal distinct similarities and differences in the interaction between lapatinib or gefitinib and EGFR/HER2.

Materials and Methods

Cell culture and transfections. Chinese hamster ovary (CHO)-K1 cells were from American Type Culture Collection (ATCC) and cultured in Ham's F12 medium (Invitrogen) supplemented with 10% fetal bovine serum (FBS; Hyclone). CHO-K1 cells were seeded at 2.42×10^6 per 100-mm dish 24 h before transfection. Cells were then incubated at 37°C in a CO_2 incubator in complete medium containing 0.18 mL Lipofectamine 2000 (Invitrogen) and 12 μg plasmid DNA per dish for 24 h. EGFR and HER2 expression was confirmed by immunoprecipitation/Western analyses. Human NSCLC cell lines NCI H1975, NCI H1650, NCI H1734, NCI H358, NCI H322, NCI H1781S, Calu-3, and A549 were obtained from the ATCC. All NSCLC lines were cultured in RPMI 1640 (Invitrogen) supplemented with 10% FBS.

Lapatinib and gefitinib treatment. Lapatinib and gefitinib were synthesized as described (28, 29). Transfected CHO-K1 cells were exposed to lapatinib or gefitinib at increasing concentrations (0, 0.14, 0.41, 0.12, 0.37, 1.1, and 3.3 μmol/L). Compounds were prepared in DMSO and diluted in complete medium before dosing. Cells transfected with EGFR constructs were exposed to drug for 4 h and stimulated with 10 ng/mL EGF for 10 min before cell lysis. Cells transfected with HER2 constructs were exposed to drug for 4 h and then immediately harvested for cell lysate.

Immunoprecipitation and immunoblotting. EGF was from Sigma. The anti-EGFR antibody for Western detection (αEGFR monoclonal antibody-12) and the anti-EGFR antibody for immunoprecipitation (αEGFR EGFR Ab-13) were from Lab Vision. The antiphosphotyrosine antibody αPT-66 was from Sigma. The peroxidase-conjugated anti-mouse IgG secondary antibody was from Jackson ImmunoResearch Laboratories. The anti-HER2 antibody for Western detection (αHER2 C-18) was from Santa Cruz. The anti-HER2 antibody for immunoprecipitation (αHER2 Ab-4 Clone N12) was from Lab Vision. The Alexa Fluor antibody for secondary detection of HER2 was from Invitrogen. Cell lysis, immunoprecipitation, and immunoblotting were performed as described previously (25).

Cellular growth inhibition studies. The NSCLC cell lines were plated in 100 μL of growth medium in 96-well tissue culture plates at the following densities: H1975, 5,000 cells per well; H1650, 10,000 cells per well; H1734, 10,000 cells per well; H358, 5,000 cells per well; H322, 5,000 cells per well; H1781S, 10,000 cells per well; A549, 4,000 cells per well; and CaLu-3, 10,000 cells per well, and the NSCLC cell lines were placed in a humidified 37°C incubator containing 5% CO_2 and 95% air, overnight. Stock solutions and compound dilutions as well as the cell proliferation studies were performed as described in the Supplementary Text. Values for the IC_{50} were determined by the method of Levenberg and Marquardt (30) with Eq. A:

$$y = V_{max} - \left(1 - \left(\frac{x^n}{K^n + x^n}\right)\right) \qquad (A)$$

PCR amplification, sequencing, and cloning. Amplification of the *EGFR* gene was performed using genomic DNA from NSCLC cell lines H358, H1734, H1975, H1650, H322, and A549 (ATCC). PCR primers were designed within flanking intronic regions to amplify coding region (exons 2–28) in the *EGFR* gene (NM_005228.3). Sequence data were not obtained for exon 1 in any cell line due to high guanine-cytosine content. Primer pairs used for *EGFR* amplification are listed in Supplementary Table S1. For direct sequencing of amplicons, all sequence-specific forward primers were tailed with the universal M13 forward primer sequence (5′-TGTAAAACGACGGCCAGT-3′), and all sequence-specific reverse primers were tailed with the universal M13 reverse primer sequence (5′-CAGGAAACAGCTATGACC-3′).

Sequence analysis of the *HER2* (NM_004448.2) gene tyrosine kinase domain (exons 18–24) was accomplished using genomic DNA from NSCLC cell lines H1781S and Calu-3 (ATCC). Intron-based primers used for PCR amplification of the *HER2* tyrosine kinase domain were reported by Shigematsu et al. (22) and are listed in Supplementary Table S3. See Supplementary Text for detailed PCR and sequencing protocols and for description of cloning and expression of EGFR and HER2 mutants.

Structural modeling. Due to the different EGFR conformations observed in the erlotinib and lapatinib crystal structures, mutations were considered in the context of both the active and inactive-like conformations. Models were constructed in both conformations for each mutant and examined for interactions that would stabilize or destabilize inhibitor binding. Coordinates from PDB1m17 and PDB1xkk were used as the starting models for the active and inactive conformations of EGFR. It was assumed that gefitinib would bind to the same conformation of the protein as erlotinib.

Enzyme kinetic analysis: determination of catalytic rates V_{max} and $K_m^{(app)}$ for ATP-Mg. V_{max} and $K_m^{(app)}$ for ATP-Mg were determined at a fixed concentration of peptide substrate and variable concentrations of ATP-Mg. The constructs of the enzyme were based on the intracellular domain of EGFR (amino acids 671–1210). Enzyme purification and kinase reaction conditions were as described by Brignola et al. (31). Briefly, phosphorylated product was detected using 1 μCi [γ-^{33}P]ATP per reaction and the phosphocellulose product detection method. Reaction buffers contained 50 mmol/L 3-(*N*-morpholino) propane sulfonic acid (pH 7.5), 10 mmol/L $MgCl_2$, 0.01% Tween 20, 1 mmol/L DTT, and 100 nmol/L enzyme. Incubations were at 23°C. The peptide substrate, biotin-(amino-hexanoic acid)-EEEEYFELVAKKK-CONH2, was used at a fixed concentration of 100 μmol/L. Eleven concentrations of ATP-Mg were used ranging from 4 to 300 μmol/L. For each substrate concentration, initial rates were determined from the linear portion of a 30-min time course sampled at 0, 10, 20, and 30 min. In all cases, product formation was <10% of the initial ATP substrate and <20% of the peptide substrate. V_{max} and $K_m^{(app)}$ values were estimated from these experiments by fitting the data to Eq. B:

$$v = \frac{V_{max}(\mathrm{ATP})}{K_m^{app} + (\mathrm{ATP})}. \qquad (B)$$

The fraction of a protein sample that is catalytically competent often varies for mutant and wild-type or for different preparations of the same enzyme. Therefore, to compare the catalytic activity of mutant enzymes with each other and the wild-type enzyme, it is important to have an independent measure of the fraction of the enzyme preparation that is catalytically competent. The active fraction for enzymes is usually assumed to be equal to the fraction of the preparation capable of binding a potent inhibitor that binds in the active site. This value was obtained directly from K_i determinations for lapatinib and gefitinib (E in Eq. C below), and was used to calculate V_{max}. For wild-type EGFR and all of the EGFR point mutations, the active fraction of the protein was between 80% and 100%. For EGFR del15, ~10% of total protein was active.

Estimation of K_i for lapatinib and gefitinib. K_i values for lapatinib and gefitinib were estimated for wild-type and mutant EGFR using second-order assumptions because these enzyme-inhibitor complexes exhibit tight-binding behavior. Reactions were carried out with variable inhibitor concentration at several fixed enzyme concentrations. The lapatinib-EGFR interaction also exhibits significant time-dependent (or slow-binding) behavior. However, a 30-min preincubation period was sufficient to allow EGFR-lapatinib binding to reach equilibrium under the conditions of these experiments. For the EGFR-gefitinib complex, a 5-min preincubation was sufficient because binding reaches equilibrium more quickly than for the EGFR-lapatinib complex.

The concentration range for each EGFR-inhibitor pair used in this analysis was independently selected to optimize the accuracy of the K_i estimate. For each experiment, six fixed concentrations of enzyme were used that ranged up to six times the initial concentration. The initial nominal concentration used for each enzyme was as follows: wild-type, 8 nmol/L; L861Q, 8 nmol/L; G719C, 10 nmol/L; Δ746–750, 40 nmol/L; and L858R, 7 nmol/L. Thus, for wild-type EGFR, the six nominal concentrations used were 8, 16, 24, 32, 40, and 48 nmol/L. A very similar concentration range was used for all EGFR variants except Δ746–750, which was used at a significantly higher nominal concentration because a relatively small fraction of this enzyme variant was capable of binding the inhibitor (see Results). Eleven concentrations of inhibitor were used evenly, spanning concentrations from 10-fold lower than the apparent IC_{50} to 10-fold higher than the apparent IC_{50}.

The rate of product formation was determined using the phosphocellulose filter–binding method (31). The concentration of ATP-Mg was 20 μmol/L, the concentration of peptide, biotin-(aminohexanoic acid)-EEEEYFELVAKKK-CONH2, was 100 μmol/L, and the time of incubation was 20 min. Each experimental condition was performed in quadruplicate, and the average rate of product formation was determined. Reaction rates were expressed as a percentage of the no-inhibitor control reaction for each concentration of enzyme used. K_i^{app} estimates were obtained according to the general method described by Morrison (32) by globally fitting the data to Eq. C:

$$v_i = v_o \times 1 - \frac{(a[E] + [I] + K_i^{app}) - \sqrt{(a[E] + [I] + K_i^{app})^2 - 4a[E][I]}}{2a[E]} + B \quad (C)$$

where the experimental variable a is the factor from 1 to 6 representing the incremental increase in the volume of enzyme used and $[I]$ is the concentration of inhibitor. For experimental results, v_i is the initial rate of product formation normalized to the control value in the absence of inhibitor. For curve fit variables, v_o is the uninhibited rate of the reaction (maximum asymptote of the inhibition curve), B is the residual rate of catalysis at saturating concentrations of inhibitor (minimum asymptote of the inhibition curve), E is the concentration of enzyme at $a = 1$, and $K_i^{(app)}$ is the apparent K_i estimated from the experiment.

$K_i^{(app)}$ values can be converted to K_i values because the inhibitors are competitive with ATP. The equation that explains this relationship is as follows (33):

$$K_i^{(app)} = K_i\left(1 + \frac{[ATP]}{K_m^{(app)}}\right). \quad (D)$$

Results

Truncated forms of EGFR, HER2, HER3, and HER4 have been crystallized as apo proteins or as binary complexes. The binary complex structures include inhibitors that target the intracellular kinase domain or antibodies that bind the extracellular domain (24, 34–41). From these structures, it is apparent that EGFR is capable of relatively large conformational changes upon inhibitor or ligand binding. Recent cocrystal structures of EGFR-erlotinib or EGFR-lapatinib are very different from one another. EGFR-erlotinib has a structure very similar to apo-EGFR. We assume that gefitinib binds in a similar fashion. In contrast, lapatinib binding to EGFR involves several structural changes (24, 41). The EGFR-lapatinib structure suggested that lapatinib binding may be affected by some of the common NSCLC mutations. This report is focused on the following seven EGFR variants, which are found in human NSCLC tumors: Δ746-750 (del15), Δ746-753S (del18), G719C, G719S, L858R, L861Q, and T790M. Four HER2 mutants, YVMA, G776VinsC, H878Y, and V659E, were also characterized in this study.

Kinetic analysis of tyrosine kinase activity of wild-type and mutant EGFR. To understand the effect of specific EGFR mutations on EGFR tyrosine kinase activity, the kinetic variables of EGFR variants were determined using an *in vitro* kinase assay. For these experiments, the intracellular domains of wild-type EGFR and the mutants were expressed in insect cells using a baculovirus expression system, and mutant and wild-type proteins were purified to ~80% homogeneity. The apparent K_m and V_{max} values for ATP-Mg were determined for wild-type and mutant EGFR at a fixed concentration of peptide substrate (Table 1). Wild-type EGFR had a V_{max} of 0.52 mol/min/mol. All EGFR mutants in this study had higher intrinsic catalytic activity than wild-type EGFR. L861Q and L858R were the most active (23- and 17-fold higher V_{max} than that for wild-type EGFR, respectively). The V_{max} for G719C and del15 was 4- and 29-fold higher than that for wild-type EGFR, respectively. At present, the mechanism for this activation is not known; however, all the EGFR mutants characterized here have a higher K_m for ATP-Mg than wild-type EGFR.

Table 1. Biochemical properties of EGFR mutants

Protein	Catalytic activity		Lapatinib inhibition		Gefitinib inhibition	
	V_{max}	$K_m^{(app)}$ ATP	K_i	$t_{1/2}$	K_i	$t_{1/2}$
	(mol/min/mol)	(μmol/L)	(nmol/L)	(min)	(nmol/L)	(min)
Wild-type	0.52 ± 0.01	9 ± 0.9	0.10 ± 0.02	224	0.19 ± 0.11	9
del15	15 ± 1	118 ± 20	15.01 ± 0.13	18	0.07 ± 0.01	18
L861Q	12.4 ± 0.6	55 ± 6	0.42 ± 0.18	nd	0.12 ± 0.01	nd
G719C	2.2 ± 0.2	97 ± 16	0.70 ± 0.04	nd	0.94 ± 0.14	nd
L858R	8.6 ± 0.2	55 ± 3	3.05 ± 0.75	56	0.20 ± 0.05	9.4

NOTE: Values are the average of at least three independent experiments ± SD.
Abbreviation: nd, not determined.

Estimation of mutant and wild-type K_i for lapatinib and gefitinib. The estimation of K_i for lapatinib and gefitinib is complicated because EGFR exhibits slow-binding and tight-binding characteristics with these inhibitors. The EGFR-lapatinib interaction is defined as slow-binding because it takes a relatively long time for the protein and inhibitor to reach equilibrium at the concentrations used in the studies (24). The EGFR interaction with either inhibitor is defined as tight binding because the K_i values are below the concentration of the enzyme needed to catalyze the formation of measurable amounts of product. Under these conditions, the enzyme-inhibitor interaction is no longer first order, and K_i must be determined using relatively complicated experiments and data analysis methods. To account for this kinetic behavior, we determined K_i using the general analytic method described by Morrison (32), incorporating an enzyme-inhibitor preincubation to allow the system to reach equilibrium before initiating the reaction with substrate (31).

The K_i for the lapatinib interaction with wild-type and EGFR del15 was determined (Fig. 1*A* and *B*). With wild-type EGFR, increasing the concentration of enzyme used in the assay results in a shift in the apparent IC_{50}. This occurs because the K_i^{app} for the inhibitor is below the concentration of enzyme, and the apparent IC_{50} is increased arithmetically by a factor of [Enzyme]/2 (33). With EGFR del15, there is no shift in the apparent IC_{50} with increasing concentrations of enzyme. This occurs because the K_i^{app} value is above the highest concentration of enzyme used in the experiment. A global fit of these data to Eq. C gives accurate estimates of both the K_i^{app} value and the concentration of enzyme competent for inhibitor binding. Lapatinib and gefitinib have been shown to be competitive with ATP (24). Therefore, the K_i^{app} values can be converted to K_i values using Eq. D. The results showed that the K_i of lapatinib for wild-type EGFR is 0.10 nmol/L; in contrast, the K_i of lapatinib for EGFR del15 is 15 nmol/L, indicating a 150-fold decrease in the affinity of lapatinib for EGFR. The K_i of EGFR L858R is 30-fold higher than wild-type EGFR, whereas the K_i values of G719C and L861Q are slightly higher than wild-type EGFR. Lapatinib inhibition of EGFR and ErbB2 is time-dependent due to a very slow off rate compared with other quinazoline inhibitors such as gefitinib (24). The off rate of lapatinib for the mutant EGFR proteins was determined (Fig. 1*C* and *D*). We found that the increase in K_i observed with del15 and L858R corresponded to a significant decrease in the EGFR-lapatinib half-life (Table 1). The effects of these mutations on the K_i values for gefitinib are less pronounced (Table 1): the K_i values of EGFR del15 and G719C are slightly lower than for wild-type EGFR, whereas the other mutations have little or no effect on the K_i for the drug.

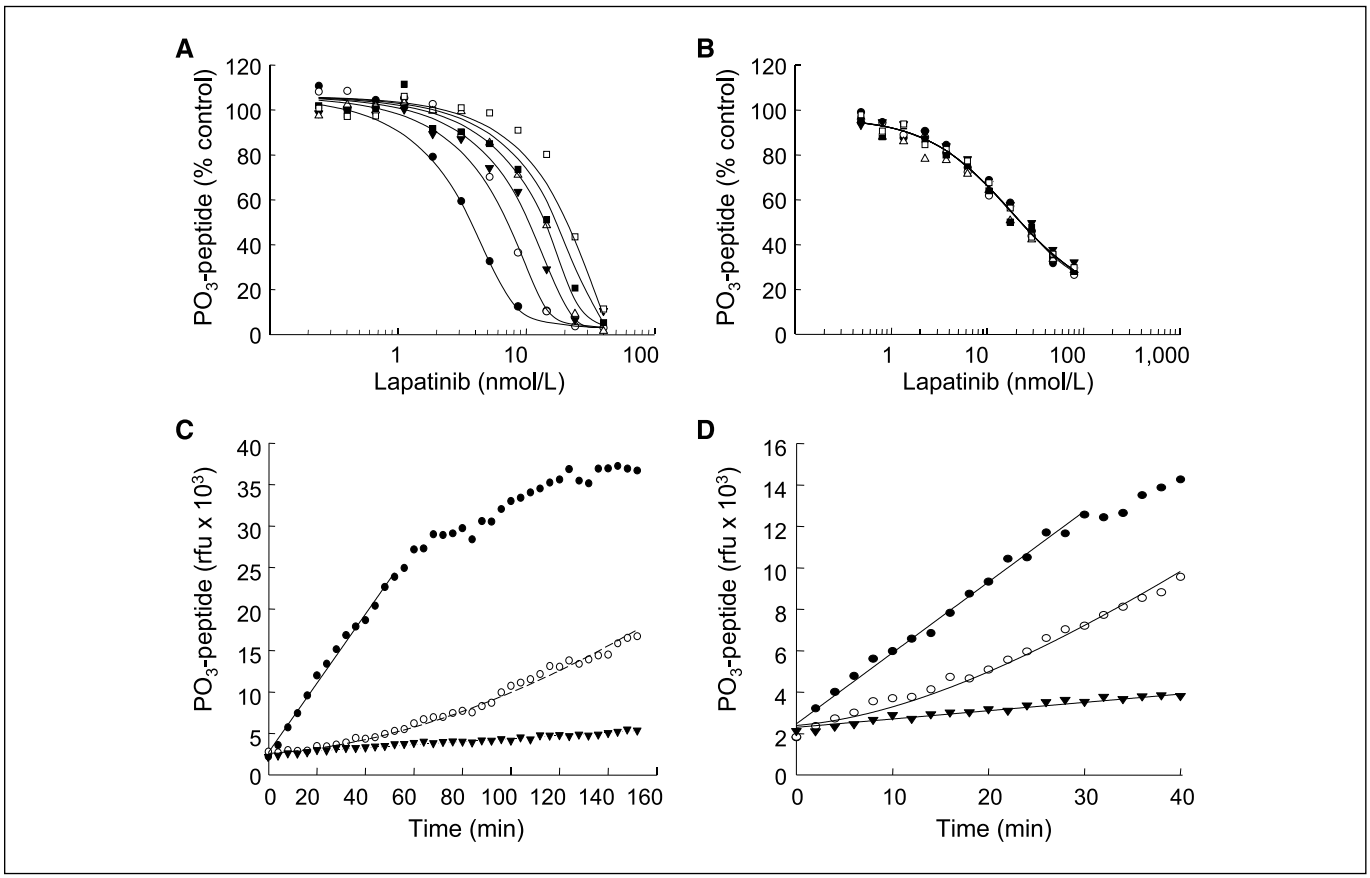

Figure 1. Lapatinib K_i^{app} and off rate for wild-type and mutant EGFR. *A,* lapatinib K_i^{app} for wild-type EGFR. Inhibition curve was determined at the following nominal concentrations of EGFR: ●, 8; ○,16; ▼, 24; △, 32; ■, 40; and □, 48 nmol/L. K_i^{app} was estimated as described in Materials and Methods. *Lines,* a global fit of the data to Eq. A. *B,* lapatinib K_i^{app} for EGFR del15. Experiment and analysis as in *A* using 40 nmol/L (●), 80 (○), 120 (▼), 160 (△), 200 (■), and 240 (□) nmol/L nominal enzyme concentration. *C,* recovery of enzyme activity after dilution of a preformed EGFR-lapatinib complex. ●, residual inhibition control. The EGFR-lapatinib complex was not preformed. Lapatinib was added to the reaction at the final diluted concentration of 0.5 nmol/L. ○, lapatinib and EGFR (0.5 μmol/L of each) were preincubated to form a complex. The reaction was initiated by diluting this complex 1,000-fold into substrate (final concentration, 0.5 nmol/L each). ▼, full inhibition control. Lapatinib and EGFR (0.5 μmol/L of each) were preincubated to form a complex. This mixture was diluted 1,000-fold into substrate mix containing 0.5 μmol/L lapatinib. Off rates were estimated from these results by fitting the data to Eq. B. *D,* off rate for lapatinib and EGFR del15. Experiment and analysis as in *C*.

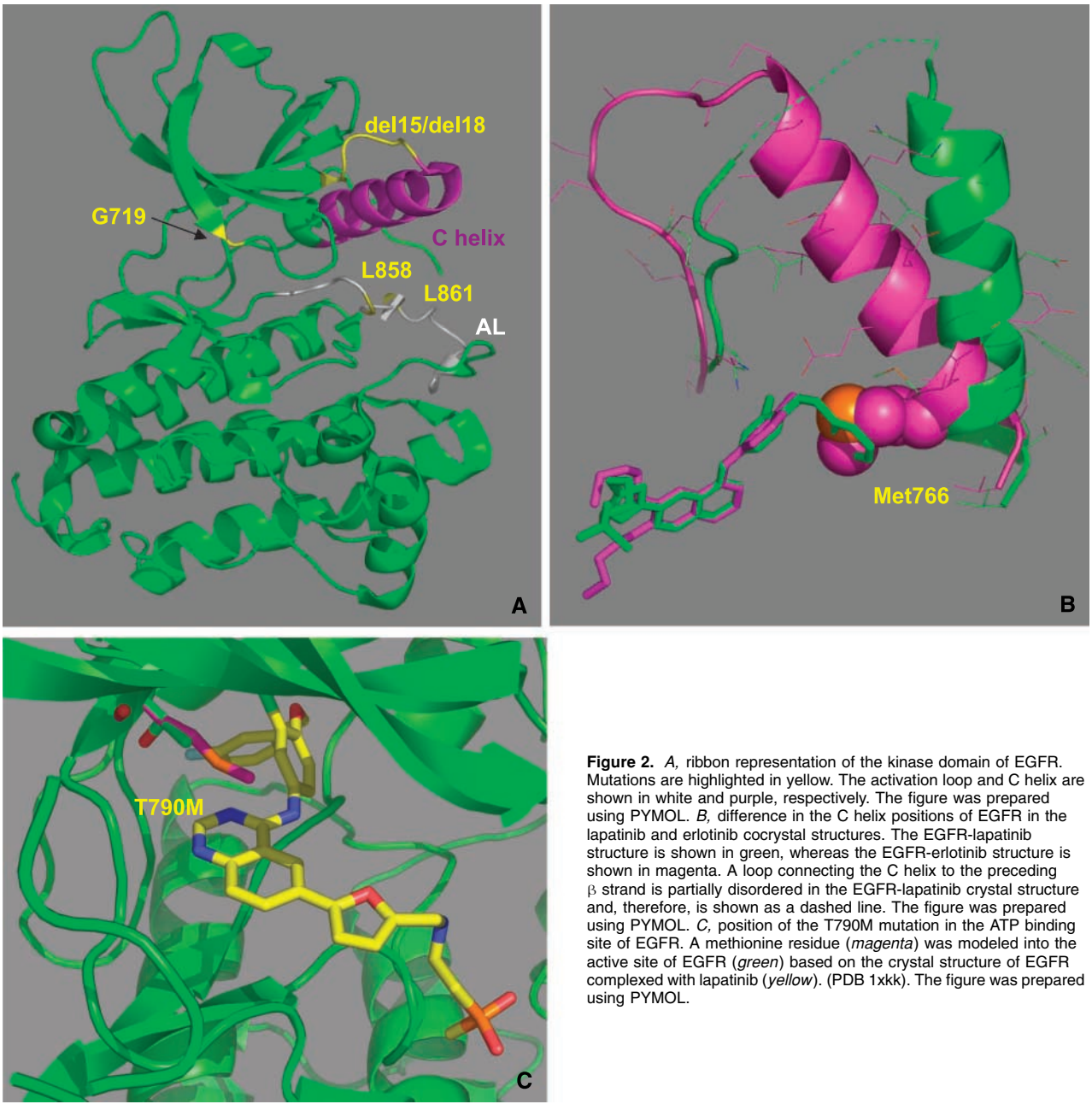

Figure 2. *A,* ribbon representation of the kinase domain of EGFR. Mutations are highlighted in yellow. The activation loop and C helix are shown in white and purple, respectively. The figure was prepared using PYMOL. *B,* difference in the C helix positions of EGFR in the lapatinib and erlotinib cocrystal structures. The EGFR-lapatinib structure is shown in green, whereas the EGFR-erlotinib structure is shown in magenta. A loop connecting the C helix to the preceding β strand is partially disordered in the EGFR-lapatinib crystal structure and, therefore, is shown as a dashed line. The figure was prepared using PYMOL. *C,* position of the T790M mutation in the ATP binding site of EGFR. A methionine residue (*magenta*) was modeled into the active site of EGFR (*green*) based on the crystal structure of EGFR complexed with lapatinib (*yellow*). (PDB 1xkk). The figure was prepared using PYMOL.

In this study, we have estimated lapatinib K_i for wild-type EGFR to be 0.1 nmol/L. In a previous publication (24), we used a different method to estimate the K_i that generated a value of 3 nmol/L. In the previous study, we did not include an enzyme inhibitor preincubation. Thus, the estimate was higher because the system had not reached equilibrium during the course of the experiment. Because of the significant time dependence of lapatinib binding, we believe that the method presented herein better estimates the affinity of the drug.

Structural modeling of mutant EGFR-inhibitor interactions. EGFR del15 and del18 were unique among the mutants studied here, in that they showed significant differential sensitivity to gefitinib and lapatinib. These mutants have deletions in the flexible loop (residues 748–754) that connects the C helix with strand 3 of the β-sheet in the NH_2-terminal lobe (Fig. 2*A*). In the EGFR-lapatinib structure, the NH_2 terminus of the C helix is shifted ~9 Å relative to its position in the apo or erlotinib structures, and this shift accommodates the larger 3-fluorobenzyl-oxy substituent in lapatinib (Fig. 2*B*). It is possible that this shift at the NH_2 terminus of the C helix is accommodated by the flexible loop, and that the shift cannot occur in EGFR mutants with a deletion in this loop. Thus, the active conformation of the C helix might be stabilized in EGFR del15 and del18, such that gefitinib binding would be favorable over lapatinib binding due to steric hindrance of the bulky head group on lapatinib.

EGFR L858R also showed a slight differential sensitivity to lapatinib and gefitinib. L858 is located on the EGFR activation

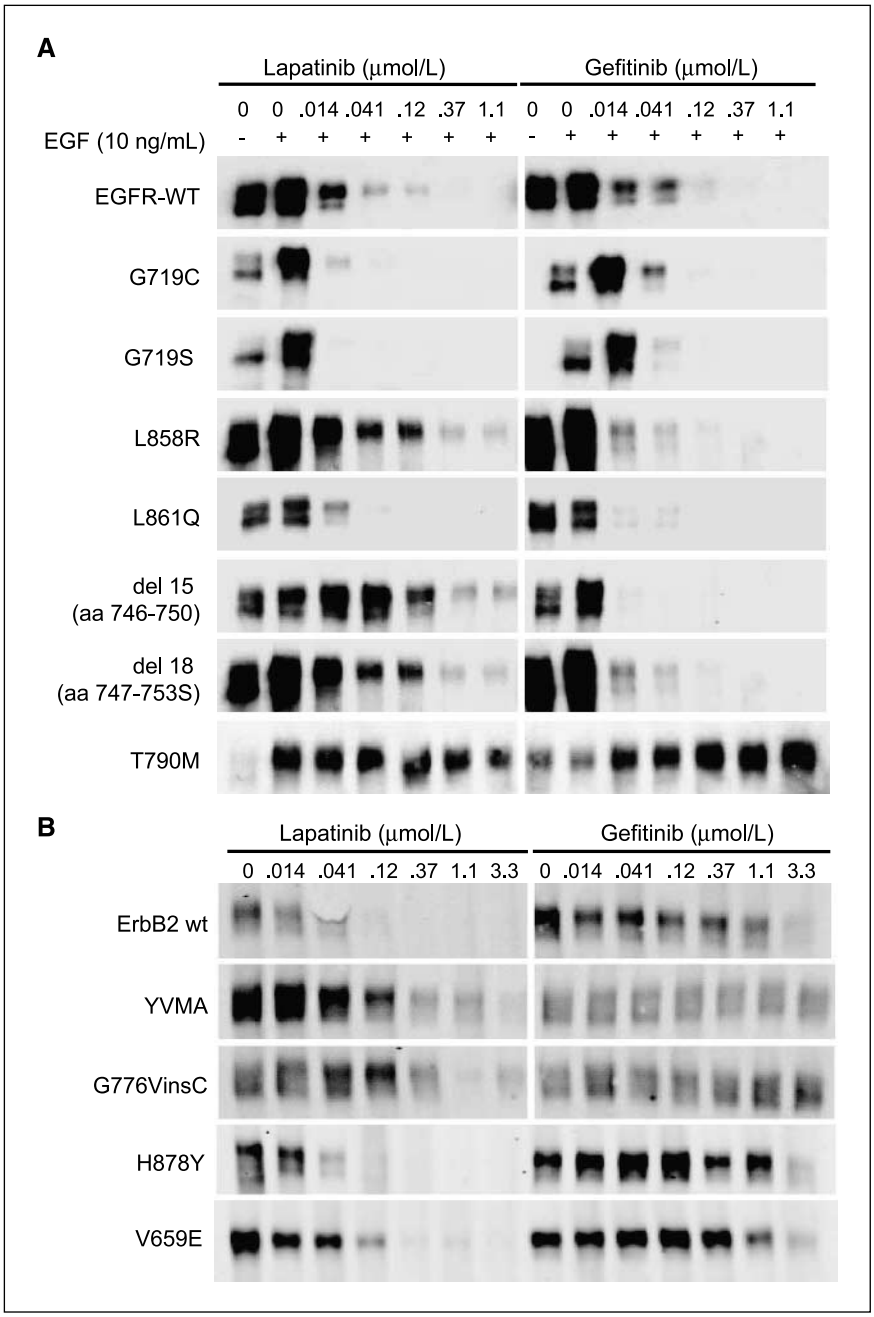

Figure 3. Inhibition of receptor autophosphorylation by lapatinib and gefitinib. *A,* CHO-K1 cells were transiently transfected with wild-type (*wt*) or mutant EGFR or HER2 constructs as indicated. Cells transfected with EGFR constructs were incubated with the indicated concentrations of lapatinib or gefitinib for 4 h, stimulated with 10 ng/mL EGF for 10 min, and lysed in radioimmunoprecipitation assay buffer buffer and immunoprecipitated with anti-EGFR antibody. Cells transfected with HER2 constructs were exposed to drug for 4 h and immunoprecipitated with anti-HER2 antibody. Western blot analysis and quantification was carried out using antiphosphotyrosine antibody PT-66 as described in Materials and Methods. Western quantification values are shown in Table 2 and represent at least two independent experiments.

loop (Fig. 2*A*). In the crystal structures of apoEGFR and EGFR-erlotinib, the hydrophobic side chain of L858 points toward a charged and polar region of the substrate-binding cleft. Mutation of this residue to arginine did not lead to any structural perturbations in the active conformation of EGFR L858R complexed with gefitinib (42). In the crystal structure of EGFR-lapatinib, the side chain of L858 forms part of the back pocket that binds the 3-fluorobenzyl-oxy substituent. Mutation of L858 to R could influence the shape and size of the back pocket. However, because the side chain of L858 is solvent exposed in the EGFR-lapatinib structure, it seems from the cell and enzyme data that the arginine side chain can be accommodated. Structural studies with this mutant and related quinazoline inhibitors indicates that the arginine side chain can rotate and point out into solution (data not shown).

T790 is located at the back of the ATP binding site (Fig. 2*C*) and is often called the gatekeeper residue (43). This mutation is analogous to the T315L mutation in bcr-abl that leads to imatinib resistance (44). In the EGFR-erlotinib structure, the side chain of T790 makes a water-mediated hydrogen bond to N3 of the quinazoline. In the EGFR-lapatinib structure, the threonine side chain is rotated relative to its position in the erlotinib structure and makes a number of direct and water-mediated hydrogen bonds to the protein. Mutation of this residue to methionine is predicted to sterically block inhibitor binding because the methionine side chain would occupy part of the same space as the quinazoline ring for both inhibitors (45).

The last three EGFR mutations examined in this study, G719C, G719S, and L861Q, have moderate effects on the K_i for lapatinib or gefitinib. Thus, it is unlikely that G719 or L861 play significant roles

in inhibitor binding. Structural modeling suggested that G719C might sterically interact with the ribose ring of ATP, perhaps explaining the observation that the K_m for ATP is ~10-fold higher for EGFR719C than for wild-type EGFR.

Inhibition of wild-type and mutant receptor autophosphorylation by lapatinib in CHO cells. The effects of EGFR mutations on EGFR activity in cells were tested by overexpressing each EGFR variant in CHO cells in the presence or absence of lapatinib or gefitinib. Cultures were exposed to EGF to activate receptor kinase activity, EGFR was immunoprecipitated from cell extracts, and EGFR autophosphorylation was measured by quantitative Western blot analyses with an antiphosphotyrosine antibody. The results show that the sensitivity to lapatinib and gefitinib is similar for wild-type EGFR and EGFR point mutants G719C, G719S, and L861Q (Fig. 3 and Table 2). The only point mutant that is differentially sensitive to either drug is L858R, which seems to be slightly more sensitive to gefitinib than wild-type EGFR and has about the same sensitivity to lapatinib as wild-type EGFR. In contrast, the two EGFR deletion mutants, del15 and del18, are much less sensitive to lapatinib inhibition than wild-type EGFR. Gefitinib inhibits these deletion mutants with better potency than wild-type EGFR. Interestingly, T790M is resistant to inhibition by both drugs. These results are in general agreement with the biochemical results described above.

Recent studies identified several *HER2* mutants expressed in tumor cells from female never-smoker Asian NSCLC patients (22). The most common variants observed were HER2 YVMA and HER2 G776VinsC. The latter variant is also expressed in human NCI cell line H1781. These two variants were overexpressed in CHO cells, and receptor autophosphorylation was measured in the presence and absence of lapatinib and gefitinib (Fig. 3*B* and Table 2). Wild-type HER2 is very sensitive to lapatinib inhibition, but not to gefitinib inhibition, as expected. However, HER2 YVMA and HER2 G776VinsC are less susceptible to inhibition by either lapatinib or gefitinib. In contrast, lapatinib was a potent inhibitor (25–50 nmol/L) of receptor autophosphorylation of the point mutation HER2 H878Y, which has been described in hepatomas and the activating point mutation HER2 V659E when expressed in CHO cells (Table 2).

Table 2. EGFR and HER2 mutant–dependent inhibition of autophosphorylation in CHO cells

Cell line	IC_{50} (nmol/L) immunoblot	
	Lapatinib	Gefitinib
EGFR wild-type	22 ± 13	44 ± 25
EGFR G719C	<14	<14
EGFR G719S	<14	<14
EGFR L858R	24 ± 14	<14
EGFR L861Q	<14	<14
EGFR del15	361 ± 119	<14
EGFR del18	155 ± 25	<14
EGFR T790M	>3,300	>2,600
HER2 wild-type	87 ± 107	2,120 ± 1,410
HER2 YVMA	20, 78, and 80% inhibition at 3,300*	>3,300
HER2 G776VinsC	20, 69, and 77% inhibition at 3,300*	20, 40% inhibition at 3,300*
HER2 H878Y	26 ± 10	2,110 ± 1,510
HER2 V659E	47 ± 18	1,380 ± 1,290

NOTE: Values are the average of at least two independent experiments ± SD.
*Values are the maximum inhibition at the highest concentration tested for two or three independent experiments.

Inhibition of wild-type and mutant cell growth by lapatinib. The ability of lapatinib and gefitinib to inhibit proliferation of human NSCLC cell lines expressing wild-type or mutant EGFR was also examined. The lapatinib IC_{50} for cell growth varied up to 10-fold in four cell lines expressing wild-type EGFR (Table 3), and the reason for this variation is not understood. However, IC_{50} for cell growth was similar for lapatinib and gefitinib in each of these four cell lines. Two of these wild-type–expressing cell lines were tested for inhibition of phosphorylated EGFR (pEGFR), and both compounds were effective (Supplementary Table S1). This is consistent with the fact that lapatinib and gefitinib have similar potency for wild-type-EGFR inhibition. NSCLC cell lines expressing mutant variants of EGFR were also examined (Table 3). H1650 cells, expressing EGFR del15 and H1975 cells, which are heterozygous for EGFR L858R and T790M, were relatively resistant to lapatinib and gefitinib. These data are consistent with recently published reports examining the effect of gefitinib on the growth of NSCLC cell lines (46) and the effects of gefitinib and lapatinib on the growth of H1975 (47). H1781S cells, expressing mutant HER2 G776VinsC, were relatively insensitive to growth inhibition by both lapatinib and gefitinib, although HER2 receptor autophosphorylation is susceptible to inhibition by lapatinib (Supplementary Table S1). CaLu-3 cells, which overexpress wild-type HER2, were highly sensitive to growth inhibition by lapatinib, with an IC_{50} <100 nmol/L. Gefitinib was 4-fold less effective on that cell line (Table 3).

Discussion

Several variables contribute to the effects of ErbB family receptor mutations on receptor oncogenicity and kinase inhibitor efficacy. Listed in order of increasing complexity, these variables include the effect of the mutation on (*a*) the affinity of the drug for the receptor, (*b*) the kinetic properties of the enzyme, (*c*) receptor signaling and regulation, and (*d*) dependence of the tumor cell on the signal from the receptor.

At the simplest level, the mutations may result in changes in tyrosine kinase activity and inhibitor binding. The effect of mutations on the biochemical properties of the receptor was obtained by purifying EGFR catalytic domains and determining enzyme kinetic variables with an *in vitro* tyrosine kinase assay. The results indicate that EGFR mutations that are common in NSCLC are highly activating (Table 1). For example, the V_{max} values of EGFR L858R and del15 were 17- and 30-fold higher than for wild-type EGFR, respectively. These activating mutations may be advantageous to tumor cell growth, which may explain why they are frequently isolated in NSCLC. The mutations also affect drug affinity for EGFR. The lapatinib K_i was 150-fold higher for del15 and 30-fold higher for L858R than for wild-type EGFR. Modest effects on lapatinib K_i were observed for other mutants and on the affinity of del15 for gefitinib. The effects on inhibitor K_i can be explained by structural models derived from EGFR-inhibitor cocrystals (24, 41). Lapatinib binding seems to require a conformational change in the apo-EGFR structure, which allows the bulky anilinoquinazoline headgroup to protrude into the back pocket of the enzyme. The models suggest that EGFR deletions affecting residues 748 to 754 (del15 and del18) reduce the

Table 3. Lapatinib and gefitinib-mediated inhibition of cell growth and receptor status

Cell line	Receptor status	IC_{50} (μmol/L) lapatinib	IC_{50} (μmol/L) gefitinib
H1975	EGFR L858R/T790M	10.1 ± 1.3	6.9 ± 1.7
H1650	EGFR del15	6.9 ± 2.4	>23
H1734	EGFR wild-type	4.0 ± 1.4	5.2 ± 3.0
H358	EGFR wild-type	0.64 ± 0.09	0.52 ± 0.16
A549	EGFR wild-type	5.0 ± 0.49	4.2 ± 0.2
H322	EGFR wild-type	0.92 ± 0.02	0.48 ± 0.06
H1781S	HER2 G776VinsC	2.6 ± 0.5	5.5 ± 1.1
CaLu-3	HER2 overexpressed wild-type	0.057 ± 0.006	0.24 ± 0.01

NOTE: Values represent the average of two independent experiments ± SD.

conformational flexibility of the receptor, which may prevent the C helix from moving to accommodate lapatinib binding. Gefitinib binds to a structure very similar to apo-EGFR and does not require this sort of conformational flexibility and is not affected by these variants.

Recently, other studies comparing the biochemical properties of wild-type EGFR to EGFR harboring mutations have been published (42, 48, 49). The kinetic properties that we have measured are in general agreement with these reports. For example, all of these studies report that L858R or del15 result in an increase in K_m^{ATP} and significantly increase the catalytic activity of the enzyme. Yun et al. (42) determined the structure of EGFR L858R in complex with the ATP analogue AMP-PNP or the inhibitor, gefitinib. They found that the L858R mutation seems to stabilize the active conformation of EGFR by preventing the activation loop from adopting the inactive-like helical conformation. Presumably, these findings explain the increase in measured catalytic rate (V_{max}) of this enzyme. Yun et al. (42) also found that the structure of the EGFR-gefitinib complex is in the active-like conformation, and gefitinib binding to wild-type EGFR is identical to gefitinib binding to EGFR L858R. In spite of this structural similarity, they found that EGFR L858R binds gefitinib tighter than wild-type EGFR (K_d = 2.6 versus 53.5 nmol/L, respectively). They propose that this increase in affinity for gefitinib results from the stabilization of the active-like conformation of EGFR by the mutation. In contrast, we have obtained essentially identical K_i values for gefitinib with wild-type and L858R EGFR (K_i = 0.2nmol/L for both). Our K_i determinations were obtained by measuring substrate phosphorylation in an *in vitro* kinase assay and are similar to other such measurements of gefitinb affinity to wild-type EGFR (24, 50). Yun et al. (42) determined the inhibitor K_d by measuring changes in the intrinsic fluorescence of the EGFR protein induced by inhibitor addition. One possible explanation for these discrepancies is that fluorescent changes are induced by compound binding to the total population of EGFR molecules in solution, whereas substrate phosphorylation assays are only sensitive to inhibitor binding to the fraction of active EGFR molecules.

Because gefitinib and lapatinib compete with ATP for receptor binding, their potency in cells depends upon several factors including the receptor K_m for ATP, the concentration of ATP in the cell, and inhibitor K_i. The relationship between these variables is described by Eq. D (33).

From Eq. D it is apparent that a higher K_m^{ATP} will result in a lower IC_{50} for a kinase inhibitor in cells even if the inhibitor K_i does not change. Using these relationships, one may predict the expected IC_{50} for inhibition of receptor autophosphorylation in cells. For lapatinib, the predicted IC_{50}s for wild-type and del15 EGFR are 22 and 270 nmol/L, respectively. These numbers are in very good agreement with the measured values, 22 and 361 nmol/L, respectively.

The susceptibility of human tumor cell lines expressing EGFR mutations to lapatinib-mediated growth inhibition was also examined in this study. Interestingly, lapatinib-mediated inhibition of the growth of these cell lines did not correlate directly with biochemical and autophosphorylation data. For example, the lapatinib IC_{50} for receptor autophosphorylation was reduced to ≤40 nmol/L in cells expressing wild-type EGFR (H1734) and expressing the HER2 mutation G776VinsC (H1781S), but the lapatinib IC_{50} for cell growth was above 2 μmol/L. In addition, Wang and coworkers (51) recently reported a decrease in colony formation of H1781 tumor cells with lapatinib but at a concentration of 5 μmol/L. Furthermore, the lapatinib and gefitinib IC_{50}s for cell growth both varied up to 10-fold in four NSCLC cell lines expressing wild-type EGFR. The resistance to lapatinib shown for the H1650 cell line is not surprising because the del15 mutation reduces the affinity of lapatinib binding and pEGFR is not inhibited in these cells. The reason for the low potency of gefitinib on cell proliferation, however, is not clear, and pEGFR is effectively reduced with gefitinib treatment in these cells. This may indicate that the cell lines are not dependent on EGFR or HER2 for growth, and additional factors contribute to the susceptibility of these cells to growth inhibition by lapatinib and gefitinib.

In summary, this is the first study that we are aware of to report biochemical, structural, and biological data on the inhibition of common NSCLC EGFR and HER2 variants by a dual tyrosine kinase inhibitor. We have fully characterized the inhibition of intrinsic catalytic activity of receptor variants by lapatinib through structure-, enzyme-, and cell-based assays. Structural models of EGFR-lapatinib interactions show that the effect of EGFR mutations also depends on the magnitude of the effect on conformation and structural flexibility. In addition, cell line heterogeneity modulates the sensitivity of lapatinib in EGFR/HER2 regulation of cell growth and survival. In this study, we show that the HER2-overexpressing NSCLC cell line was most responsive to growth inhibition by lapatinib and is consistent with results from clinical trials of lapatinib in patients with HER2 overexpressing breast cancer (26, 27). The biochemical and biological data on EGFR and HER2 presented here for NSCLC highlights the complexity of receptor sensitivity and targeted therapies and shows how understanding the potency of specific tyrosine kinase inhibitors toward specific receptor variants can contribute significantly to the design, execution, and interpretation of clinical trials for these agents.

Acknowledgments

Received 6/26/2007; revised 10/19/2007; accepted 11/15/2007.

The costs of publication of this article were defrayed in part by the payment of page charges. This article must therefore be hereby marked *advertisement* in accordance with 18 U.S.C. Section 1734 solely to indicate this fact.

Conflict of interest: All authors were employees of GlaxoSmithKline at the time the work was performed.

We thank David McKee and Earnest Horne for their contributions to protein expression and purification; Hong Shi, Li Liu, and Yawei Li for technical help with HER2 mutant assays; and Miriam Sander and Francine Carrick for editorial assistance.

References

1. Traxler P. Tyrosine kinases as targets in cancer therapy - successes and failures. Expert Opin Ther Targets 2003;7:215–34.
2. Giaccone G. Epidermal growth factor receptor inhibitors in the treatment of non-small-cell lung cancer. J Clin Oncol 2005;23:3235–42.
3. Marshall J. Clinical implications of the mechanism of epidermal growth factor receptor inhibitors. Cancer 2006;107:1207–18.
4. Auberger J, Loeffler-Ragg J, Wurzer W, Hilbe W. Targeted therapies in non-small cell lung cancer: proven concepts and unfulfilled promises. Curr Cancer Drug Targets 2006;6:271–94.
5. Tibes R, Trent J, Kurzrock R. Tyrosine kinase inhibitors and the dawn of molecular cancer therapeutics. Annu Rev Pharmacol Toxicol 2005;45:357–84.
6. Baselga J. Targeting tyrosine kinases in cancer: the second wave. Science 2006;312:1175–8.
7. Mauro MJ, Druker BJ. STI571: a gene product-targeted therapy for leukemia. Curr Oncol Rep 2001;3:223–7.
8. Buchdunger E, Cioffi CL, Law N, et al. Abl protein-tyrosine kinase inhibitor STI571 inhibits *in vitro* signal transduction mediated by c-kit and platelet-derived growth factor receptors. J Pharmacol Exp Ther 2000;295:139–45.
9. Buchdunger E, Zimmermann J, Mett H, et al. Inhibition of the Abl protein-tyrosine kinase *in vitro* and *in vivo* by a 2-phenylaminopyrimidine derivative. Cancer Res 1996;56:100–4.
10. Krystal GW, Honsawek S, Litz J, Buchdunger E. The selective tyrosine kinase inhibitor STI571 inhibits small cell lung cancer growth. Clin Cancer Res 2000;6:3319–26.
11. Lynch TJ, Bell DW, Sordella R, et al. Activating mutations in the epidermal growth factor receptor underlying responsiveness of non-small-cell lung cancer to gefitinib. N Engl J Med 2004;350:2129–39.
12. Perrone F, Di Maio M, Budillon A, Normanno N. Targeted therapies and non-small cell lung cancer: methodological and conceptual challenge for clinical trials. Curr Opin Oncol 2005;17:123–9.
13. Haber DA, Bell DW, Sordella R, et al. Molecular targeted therapy of lung cancer: EGFR mutations and response to EGFR inhibitors. Cold Spring Harb Symp Quant Biol 2005;70:419–26.
14. Shigematsu H, Gazdar AF. Somatic mutations of epidermal growth factor receptor signaling pathway in lung cancers. Int J Cancer 2006;118:257–62.
15. Liu B, Bernard B, Wu JH. Impact of EGFR point mutations on the sensitivity to gefitinib: insights from comparative structural analyses and molecular dynamics simulations. Proteins 2006;65:331–46.
16. Kosaka T, Yatabe Y, Endoh H, et al. Analysis of epidermal growth factor receptor gene mutation in patients with non-small cell lung cancer and acquired resistance to gefitinib. Clin Cancer Res 2006;12:5764–9.
17. Sordella R, Bell DW, Haber DA, Settleman J. Gefitinib-sensitizing EGFR mutations in lung cancer activate anti-apoptotic pathways. Science 2004;305:1163–7.
18. Ahmed SM, Salgia R. Epidermal growth factor receptor mutations and susceptibility to targeted therapy in lung cancer. Respirology 2006;11:687–92.
19. Pao W, Miller VA, Politi KA, et al. Acquired resistance of lung adenocarcinomas to gefitinib or erlotinib is associated with a second mutation in the EGFR kinase domain. PLoS Med 2005;2:e73.
20. Sawyers C. Opportunities and challenges in the development of kinase inhibitor therapy for cancer. Genes Dev 2003;17:2998–3010.
21. Pao W, Miller V, Zakowski M, et al. EGF receptor gene mutations are common in lung cancers from "never smokers" and are associated with sensitivity of tumors to gefitinib and erlotinib. Proc Natl Acad Sci U S A 2004;101:13306–11.
22. Shigematsu H, Takahashi T, Nomura M, et al. Somatic mutations of the HER2 kinase domain in lung adenocarcinomas. Cancer Res 2005;65:1642–6.
23. Rusnak DW, Lackey K, Affleck K, et al. The effects of the novel, reversible epidermal growth factor receptor/ErbB-2 tyrosine kinase inhibitor, GW572016, on the growth of human normal and tumor-derived cell lines *in vitro* and *in vivo*. Mol Cancer Ther 2001;1:85–94.
24. Wood ER, Truesdale AT, McDonald OB, et al. A unique structure for epidermal growth factor receptor bound to GW572016 (Lapatinib): relationships among protein conformation, inhibitor off-rate, and receptor activity in tumor cells. Cancer Res 2004;64:6652–9.
25. Hegde PS, Rusnak D, Bertiaux M, et al. Delineation of molecular mechanisms of sensitivity to lapatinib in breast cancer cell lines using global gene expression profiles. Mol Cancer Ther 2007;6:1629–40.
26. Geyer CE, Forster J, Lindquist D, et al. Lapatinib plus capecitabine for HER2-positive advanced breast cancer. N Engl J Med 2006;355:2733–43.
27. Gomez HL, Chavez MA, Doval DC, et al. A phase II, randomized trial using the small molecule tyrosin kinase inhibitor lapatinib as a first-line treatment in patients with FISH-positive advanced or metastatic breast cancer. J Clin Oncol 2005;23:3046S.
28. Petrov KG, Zhang YM, Carter M, et al. Optimization and SAR for dual ErbB-1/ErbB-2 tyrosine kinase inhibition in the 6-furanylquinazoline series. Bioorg Med Chem Lett 2006;16:4686–91.
29. Barker AJ, Gibson KH, Grundy W, et al. Studies leading to the identification of ZD1839 (Iressa™): an orally active, selective epidermal growth factor receptor tyrosine kinase inhibitor targeted to the treatment of cancer. Bioorg Med Chem Lett 2001;11:1911–4.
30. Mager P, editor. Data Analysis in Biochemistry and Biophysics. New York; Academic Press; 1972.
31. Brignola PS, Lackey K, Kadwell SH, et al. Comparison of the biochemical and kinetic properties of the type 1 receptor tyrosine kinase intracellular domains. Demonstration of differential sensitivity to kinase inhibitors. J Biol Chem 2002;277:1576–85.
32. Morrison JF. Kinetics of the reversible inhibition of enzyme-catalysed reactions by tight-binding inhibitors. Biochim Biophys Acta 1969;185:269–86.
33. Copeland R. Enzymes: A practical introduction to structure, mechanism, and data analysis. NY: John Wiley and Sons; 2000. p. 309.
34. Cho HS, Leahy DJ. Structure of the extracellular region of HER3 reveals an interdomain tether. Science 2002;297:1330–3.
35. Cho HS, Mason K, Ramyar KX, et al. Structure of the extracellular region of HER2 alone and in complex with the Herceptin Fab. Nature 2003;421:756–60.
36. Ferguson KM, Berger MB, Mendrola JM, Cho HS, Leahy DJ, Lemmon MA. EGF activates its receptor by removing interactions that autoinhibit ectodomain dimerization. Mol Cell 2003;11:507–17.
37. Franklin MC, Carey KD, Vajdos FF, Leahy DJ, de Vos AM, Sliwkowski MX. Insights into ErbB signaling from the structure of the ErbB2-pertuzumab complex. Cancer Cell 2004;5:317–28.
38. Garrett TP, McKern NM, Lou M, et al. Crystal structure of a truncated epidermal growth factor receptor extracellular domain bound to transforming growth factor α. Cell 2002;110:763–73.
39. Ogiso H, Ishitani R, Nureki O, et al. Crystal structure of the complex of human epidermal growth factor and receptor extracellular domains. Cell 2002;110:775–87.
40. Shewchuk L, Hassell A, Brignola PS. ErbB4 Co-crystal. WO 2004/066921 A2; 2004; 2004.
41. Stamos J, Sliwkowski MX, Eigenbrot C. Structure of the epidermal growth factor receptor kinase domain alone and in complex with a 4-anilinoquinazoline inhibitor. J Biol Chem 2002;277:46265–72.
42. Yun C, Boggon TJ, Li Y, et al. Structures of lung cancer-derived EGFR mutants and inhibitor complexes: mechanism of activation and insights into differential inhibitor sensitivity. Cancer Cell 2007;11:217–27.
43. Liu Y, Shah K, Yang F, Witucki L, Shokat KM. Engineering Src family protein kinases with unnatural nucleotide specificity. Chem Biol 1998;5:91–101.
44. Gorre ME, Mohammed M, Ellwood K, et al. Clinical resistance to STI-571 cancer therapy caused by BCR-ABL gene mutation or amplification. Science 2001;293:876–80.
45. Blencke S, Ullrich A, Daub H. Mutation of threonine 766 in the epidermal growth factor receptor reveals a hotspot for resistance formation against selective tyrosine kinase inhibitors. J Biol Chem 2003;278:15435–40.
46. Okabe T, Okamoto I, Tamura K, et al. Differential constitutive activation of the epidermal growth factor receptor in non-small cell lung cancer cells bearing EGFR gene mutation and amplification. Cancer Res 2007;67:2046–53.
47. Carter TA, Wodicka LM, Shah NP, et al. Inhibition of drug-resistant mutants of ABL, KIT, EGF receptor kinases. Proc Natl Acad Sci U S A 2005;102:11011–6.
48. Carey KD, Garton AJ, Romero MS, et al. Kinetic analysis of epidermal growth factor receptor somatic mutant proteins shows increased sensitivity to the epidermal growth factor receptor tyrosine kinase inhibitor, erlotinib. Cancer Res 2006;66:8163–71.
49. Zhang X, Gureasko J, Shen K, Cole PA, Kuriyan J. An allosteric mechanism for activation of the kinase domain of epidermal growth factor receptor. Cell 2006;125:1137–49.
50. Wakeling AE, Guy SP, Woodburn JR, et al. ZD 1839 (Iressa): an orally active inhibitor of epidermal growth factor signaling with potential for cancer therapy. Cancer Res 2002;62:5749–54.
51. Wang SE, Narasanna A, Perez-Torres M, et al. HER2 kinase domain mutation results in constitutive phosphorylation and activation of HER2 and EGFR and resistance to EGFR tyrosine kinase inhibitors. Cancer Cell 2006;10:25–38.

Impact of Common Epidermal Growth Factor Receptor and HER2 Variants on Receptor Activity and Inhibition by Lapatinib

Tona M. Gilmer, Louann Cable, Krystal Alligood, et al.

Cancer Res 2008;68:571-579.